Genome-wide investigation of the dynamic changes of epigenome modifications after global DNA methylation editing

Julian Broche, Goran Kungulovski, Pavel Bashtrykov, Philipp Rathert & Albert Jeltsch

Supplementary figures and figure legends

Supplementary Tables

Supplementary Text

Supplementary figures and figure legends

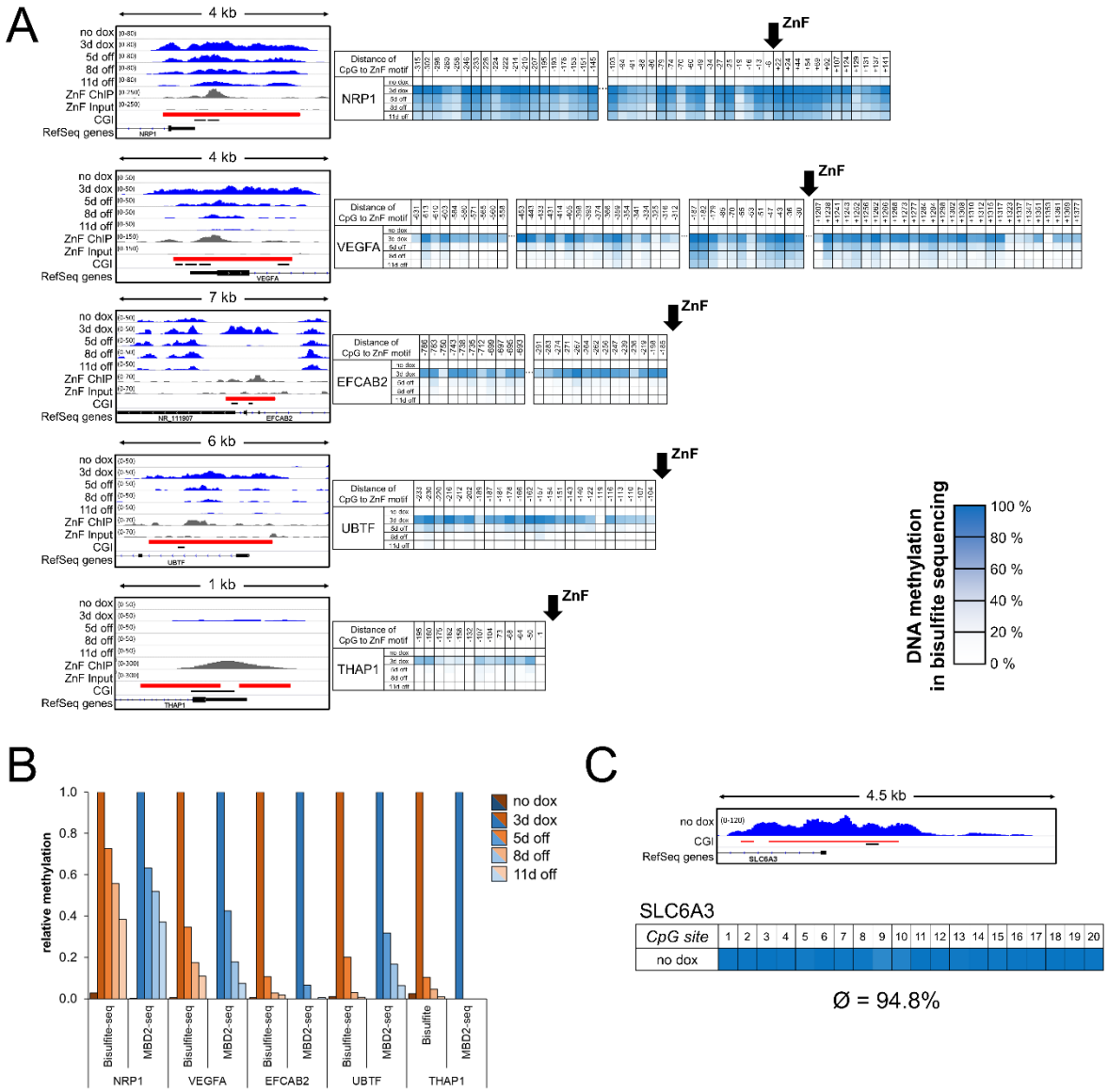

Supplementary Figure S1: Comparison of MBD2-seq data with Bisulfite-seq data in representative genomic regions. Browser views of MBD2-seq and ZnF-ChIP data in regions analyzed by Bisulfite-seq. The locations of Bisulfite amplicons are indicated as black lines below CGI. For Bisulfite-seq, data of one representative replicate are shown. (**A**) Comparison of differentially methylated CGIs in the promoters of the genes *NRP1*, *VEGFA*, *EFCAB2*, *UBTF* and *THAP1*. The relative position of ZnF binding sites is indicated with black arrows. (**B**) Comparison of Bisulfite-seq and MBD2-seq data. Average methylation levels of all CpGs in the analyzed amplicons from Bisulfite-seq were calculated and normalized to '3d dox'. The MBD2-seq signals of the whole CGIs were determined and also normalized to '3d dox'. (**C**) Exemplary, highly methylated CGI used for normalization of MBD2-seq data. Bisulfite-seq confirms the high methylation level in this region. The genomic regions shown in panel A-C are listed in Supplementary Table S6.

A

MBD2 pulldown replicates

		3AC (3d dox)		ZnF-3AC (3d dox)			no dox			Input no dox
		R1	R2	R1	R2	R3	R1	R2	R3	
3AC (3d dox)	R1	1.00	0.86	0.40	0.48	0.49	0.12	0.12	0.12	0.27
	R2	0.86	1.00	0.40	0.48	0.48	0.11	0.12	0.11	0.30
ZnF-3AC (3d dox)	R1	0.40	0.40	1.00	0.77	0.74	0.10	0.12	0.11	0.14
	R2	0.48	0.48	0.77	1.00	0.79	0.10	0.12	0.12	0.16
	R3	0.49	0.48	0.74	0.79	1.00	0.10	0.12	0.12	0.14
no dox	R1	0.12	0.11	0.10	0.10	0.10	1.00	0.67	0.62	0.00
	R2	0.12	0.12	0.12	0.12	0.12	0.67	1.00	0.62	0.01
	R3	0.12	0.11	0.11	0.12	0.12	0.62	0.62	1.00	0.00
Input no dox		0.27	0.30	0.14	0.16	0.14	0.00	0.01	0.00	1.00

		5d off			Input no dox
		R1	R2	R3	
5d off	R1	1.00	0.76	0.77	0.05
	R2	0.76	1.00	0.81	0.05
	R3	0.77	0.81	1.00	0.04
Input no dox		0.04	0.05	0.04	1.00

		8d off			Input no dox
		R1	R2	R3	
8d off	R1	1.00	0.78	0.79	0.02
	R2	0.78	1.00	0.75	0.04
	R3	0.79	0.75	1.00	0.04
Input no dox		0.02	0.04	0.04	1.00

		11d off			Input no dox
		R1	R2	R3	
11d off	R1	1.00	0.84	0.80	0.03
	R2	0.84	1.00	0.80	0.02
	R3	0.80	0.80	1.00	0.02
Input no dox		0.03	0.02	0.02	1.00

B

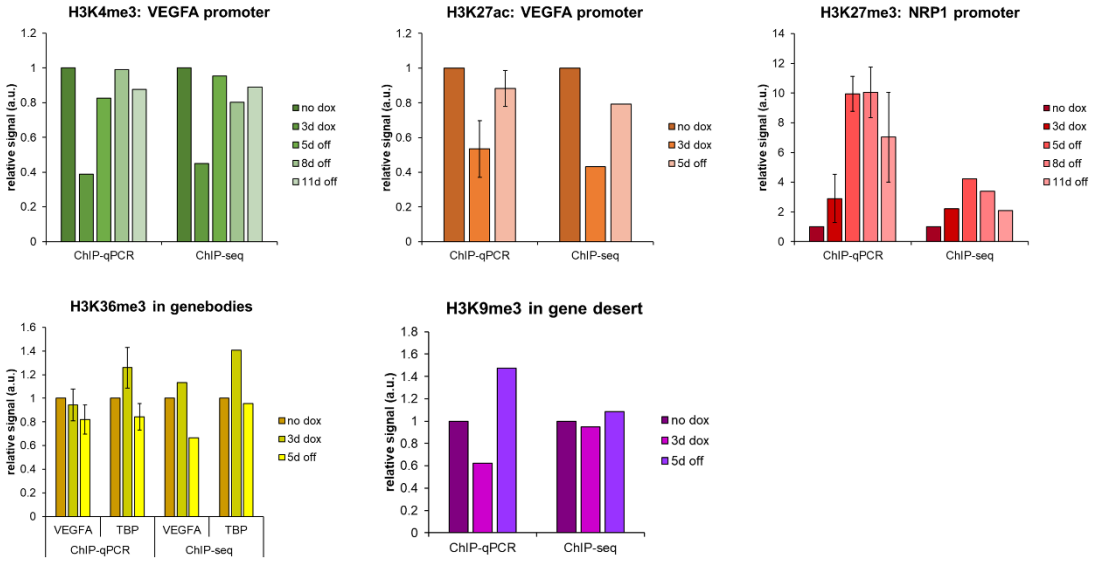

Supplementary Figure S2: Quality control of MBD2-seq and ChIP-seq data. (**A**) Calculation of Pearson correlation coefficients for MBD2-seq replicates. Experimental replicates are designated R1 to R3. Only signals in CGIs unmethylated at 'no dox' were used for this analysis, because of the highest dynamics in these regions. Pearson correlation coefficients were calculated in Excel. (**B**) Comparison of ChIP-seq and ChIP-qPCR signals in selected loci. Each ChIP-seq dataset comprises one repeat, the ChIP-qPCR experiments for H3K27ac, H3K27me3 and H3K36me3 were performed in duplicates. Error bars represent the standard deviation between repeats. The ChIP-qPCR experiments overall reflect the dynamics observed in the ChIP-seq data analysis.

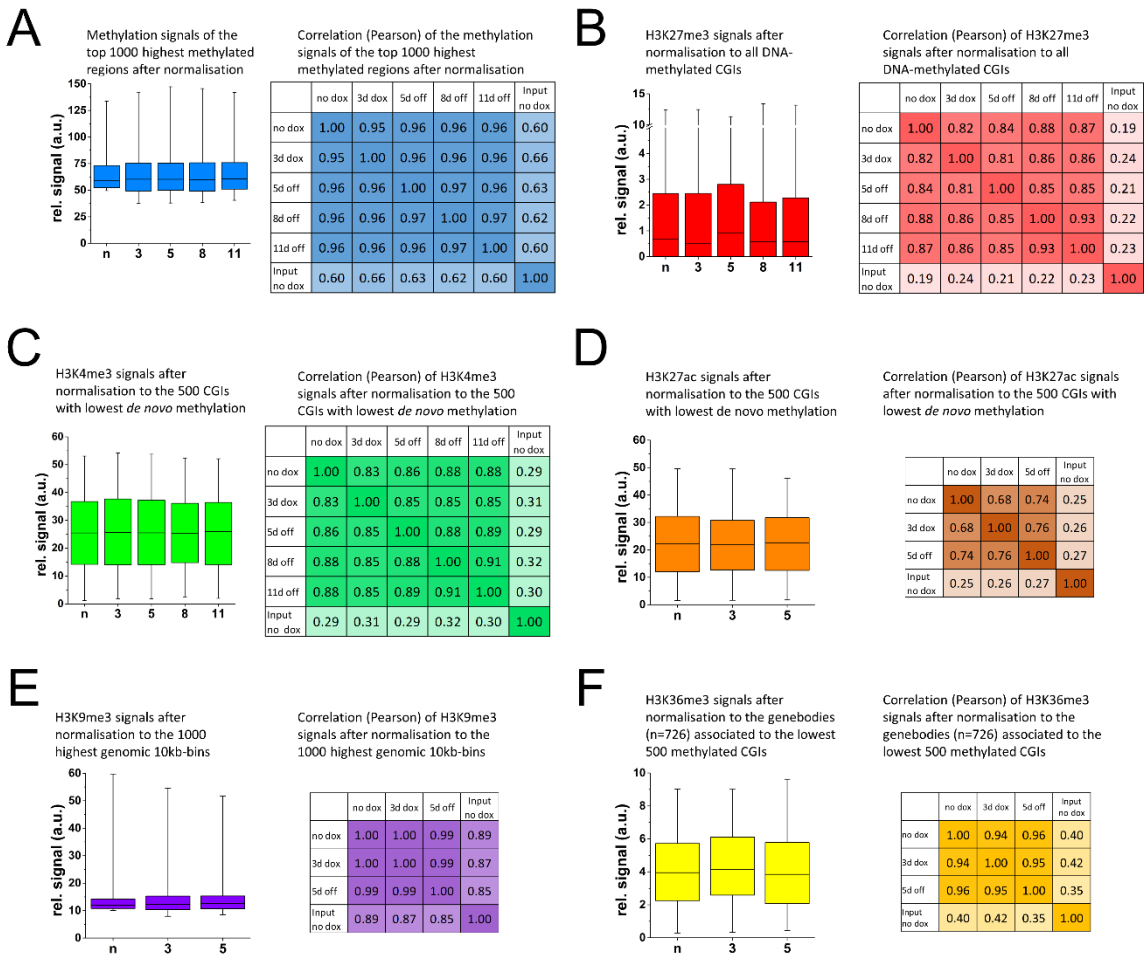

Supplementary Figure S3: Summary of the internal normalization for different epigenome modifications. (**A**) For normalization of DNA methylation signals, the signals in the 1000 CGIs showing the highest methylation at 'no dox' were used. These correspond to full methylation and should not change during the experiment. Mean signals in these CGIs were calculated and the ratios of the means compared to 'no dox' were used as scaling factors. To confirm the correct normalization, the average signals of these regions were determined after normalization. The line in the box indicates the median, the box indicates the 25th and 75th percentile, the whiskers the 5th and 95th percentile. In addition, the Pearson correlation coefficients of these regions were calculated. (**B**) For normalization of H3K27me3, the signals of all CGIs with DNA methylation at 'no dox' were used, because no DNA methylation change occurs at them, suggesting little changes of other marks. Based on these regions, scaling factors were calculated as described above. For adjustment of the background, the median signals in these CGIs were subtracted (negative values were replaced by zero). (**C**) and (**D**) For normalization of H3K4me3 and H3K27ac, the corresponding signals at 500 CGIs unmethylated at 'no dox' were used, which showed the smallest DNA methylation changes. Scaling factors for different time points were calculated as described above. (**E**) For normalization of H3K9me3, the genome was split into 10 kb bins. The mean signals in the 1000 bins showing the highest H3K9me3 signal were calculated. Scaling factors for the different time points relative to 'no dox' were obtained as described above. (**F**) For normalization of H3K36me3, the 500 CGIs gaining the least DNA methylation were associated with gene bodies (n = 726). The means of the H3K36me3 signals in these gene bodies at each time point were calculated and the ratios to 'no dox' served as scaling factors. In B-E the signals of the regions used for normalization was shown as box plot and their correlation was analyzed after the normalization as described in panel A.

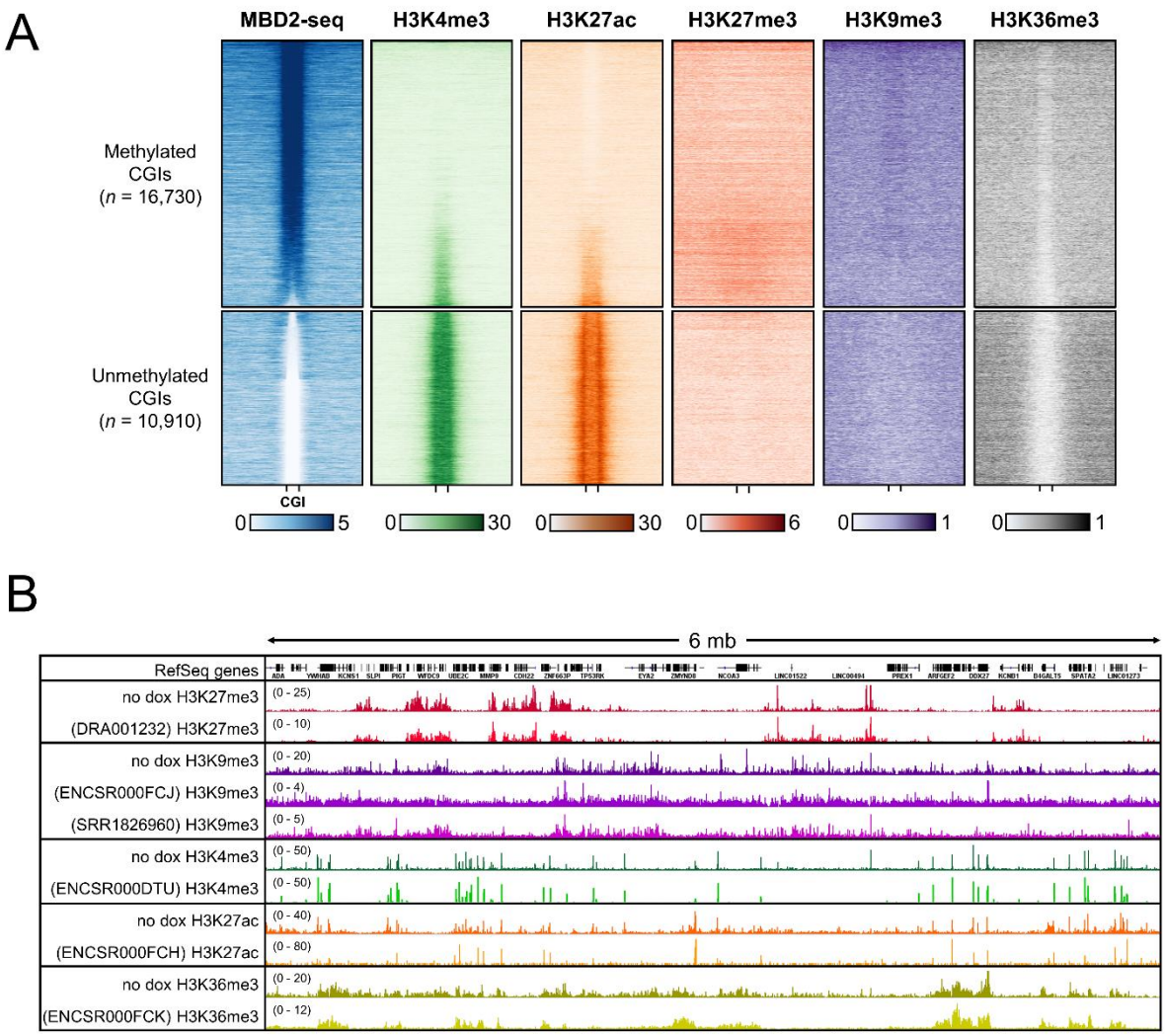

Supplementary Figure S4: Genome-wide distribution of selected histone modifications. (**A**) Heatmaps of different chromatin modifications within CGIs in uninduced cells clustered by the DNA methylation MBD2-seq signals. The heatmaps are centered around CGIs with 5 kb flanks. “Methylated” and “unmethylated” CGIs (MBD2-seq) were obtained by K-means clustering, sorted by intensity. The heatmaps of H3K4me3, H3K27ac, H3K27me3, H3K9me3, and H3K36me3 are displayed in the same order as used for MBD2-seq. (**B**) Browser view (hg19, chr20:43042127-49048811) of ChIP-seq datasets at time point ‘no dox’ in comparison with published datasets. Experiment numbers of the published data are displayed in brackets. The generated datasets display a highly similar distribution and intensity of the ChIP signals across the genome.

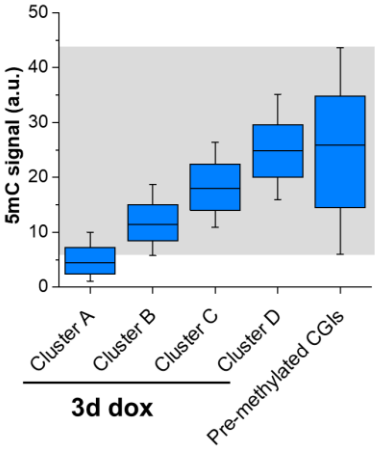

Supplementary Figure S5: Comparison of the methylation levels of clusters A-D at time point '3d dox' with the methylation levels of already methylated CGIs. Boxplots show the relative MBD2-seq signals, the line in the box indicates the median, the box indicates the 25th and 75th percentile, the whiskers the 10th and 90th percentile. The range between the 10^{th} and 90^{th} percentile of the pre-methylated CGIs is highlighted by the grey box showing the overlap with the methylation levels of clusters B-D.

A

MBD2-seq

Mean signals and confidence intervals

	no dox	3d dox	5d off	8d off	11d off
Cluster A	0.09 ± 0.01	5.12 ± 0.15	0.17 ± 0.01	0.10 ± 0.01	0.11 ± 0.01
Cluster B	0.23 ± 0.02	11.92 ± 0.23	1.71 ± 0.05	0.66 ± 0.03	0.33 ± 0.02
Cluster C	0.57 ± 0.06	18.43 ± 0.35	6.02 ± 0.16	3.19 ± 0.11	1.86 ± 0.08
Cluster D	0.55 ± 0.09	25.39 ± 0.56	14.21 ± 0.41	9.35 ± 0.33	6.51 ± 0.28

Significance of pairwise MBD2-seq differences

Cluster A

no dox	3d dox	5d off	8d off	11d off	
-	*	*	n.s.	n.s.	no dox
	-	*	*	*	3d dox
		-	*	*	5d off
			-	n.s.	8d off
				-	11d off

Cluster B

no dox	3d dox	5d off	8d off	11d off	
-	*	*	*	*	no dox
	-	*	*	*	3d dox
		-	*	*	5d off
			-	*	8d off
				-	11d off

Cluster C

no dox	3d dox	5d off	8d off	11d off	
-	*	*	*	*	no dox
	-	*	*	*	3d dox
		-	*	*	5d off
			-	*	8d off
				-	11d off

Cluster D

no dox	3d dox	5d off	8d off	11d off	
-	*	*	*	*	no dox
	-	*	*	*	3d dox
		-	*	*	5d off
			-	*	8d off
				-	11d off

B

H3K4me3

Mean signals and confidence intervals

	no dox	3d dox	5d off	8d off	11d off
Cluster A	29.90 ± 0.58	28.37 ± 0.58	29.36 ± 0.57	28.82 ± 0.54	29.81 ± 0.57
Cluster B	30.25 ± 0.61	25.83 ± 0.57	29.45 ± 0.60	28.51 ± 0.57	30.24 ± 0.61
Cluster C	29.23 ± 0.76	21.33 ± 0.64	27.63 ± 0.74	26.55 ± 0.71	28.60 ± 0.77
Cluster D	27.75 ± 0.91	14.90 ± 0.59	22.20 ± 0.84	22.73 ± 0.84	24.17 ± 0.90

Significance of pairwise H3K4me3 differences

Cluster A

no dox	3d dox	5d off	8d off	11d off	
-	*	n.s.	n.s.	n.s.	no dox
	-	n.s.	n.s.	*	3d dox
		-	n.s.	n.s.	5d off
			-	n.s.	8d off
				-	11d off

Cluster B

no dox	3d dox	5d off	8d off	11d off	
-	*	n.s.	*	n.s.	no dox
	-	*	*	*	3d dox
		-	n.s.	n.s.	5d off
			-	*	8d off
				-	11d off

Cluster C

no dox	3d dox	5d off	8d off	11d off	
-	*	*	*	n.s.	no dox
	-	*	*	*	3d dox
		-	n.s.	n.s.	5d off
			-	*	8d off
				-	11d off

Cluster D

no dox	3d dox	5d off	8d off	11d off	
-	*	*	*	*	no dox
	-	*	*	*	3d dox
		-	n.s.	*	5d off
			-	n.s.	8d off
				-	11d off

C

H3K27ac

Mean signals and confidence intervals

	no dox	3d dox	5d off
Cluster A	24.38 ± 0.53	22.97 ± 0.49	24.26 ± 0.51
Cluster B	29.91 ± 0.53	20.55 ± 0.46	23.42 ± 0.50
Cluster C	21.74 ± 0.59	17.26 ± 0.52	21.55 ± 0.60
Cluster D	19.75 ± 0.78	12.05 ± 0.57	17.98 ± 0.74

Significance of pairwise H3K27ac differences

Cluster A

no dox	3d dox	5d off	
-	*	n.s.	no dox
	-	*	3d dox
		-	5d off

Cluster B

no dox	3d dox	5d off	
-	*	n.s.	no dox
	-	*	3d dox
		-	5d off

Cluster C

no dox	3d dox	5d off	
-	*	n.s.	no dox
	-	*	3d dox
		-	5d off

Cluster D

no dox	3d dox	5d off	
-	*	*	no dox
	-	*	3d dox
		-	5d off

D

H3K27me3

Mean signals and confidence intervals

	no dox	3d dox	5d off	8d off	11d off
Cluster A	0.66 ± 0.05	0.58 ± 0.05	0.80 ± 0.05	0.41 ± 0.04	0.44 ± 0.04
Cluster B	0.78 ± 0.07	0.69 ± 0.06	0.92 ± 0.06	0.53 ± 0.06	0.60 ± 0.06
Cluster C	1.13 ± 0.12	1.11 ± 0.13	1.31 ± 0.11	1.02 ± 0.13	1.08 ± 0.14
Cluster D	3.09 ± 0.36	2.98 ± 0.32	3.56 ± 0.33	3.84 ± 0.42	3.56 ± 0.39

Significance of pairwise H3K27me3 differences

Cluster A

no dox	3d dox	5d off	8d off	11d off	
-	n.s.	*	*	*	no dox
	-	*	*	*	3d dox
		-	*	*	5d off
			-	n.s.	8d off
				-	11d off

Cluster B

no dox	3d dox	5d off	8d off	11d off	
-	n.s.	*	*	*	no dox
	-	*	*	n.s.	3d dox
		-	*	*	5d off
			-	n.s.	8d off
				-	11d off

Cluster C

no dox	3d dox	5d off	8d off	11d off	
-	n.s.	n.s.	n.s.	n.s.	no dox
	-	n.s.	n.s.	n.s.	3d dox
		-	*	n.s.	5d off
			-	n.s.	8d off
				-	11d off

Cluster D

no dox	3d dox	5d off	8d off	11d off	
-	n.s.	n.s.	n.s.	n.s.	no dox
	-	n.s.	*	n.s.	3d dox
		-	n.s.	n.s.	5d off
			-	n.s.	8d off
				-	11d off

Supplementary Figure S6: Confidence intervals and significance of pairwise differences for the analyzed chromatin modifications. (**A**) MBD2-seq, (**B**) H3K4me3, (**C**) H3K27ac and (**D**) H3K27me3. Confidence intervals for the mean signals in the clusters were calculated with Excel using an alpha value of 0.01. *, significant difference due to non-overlapping confidence intervals; n.s., not significant difference due to overlapping confidence intervals.

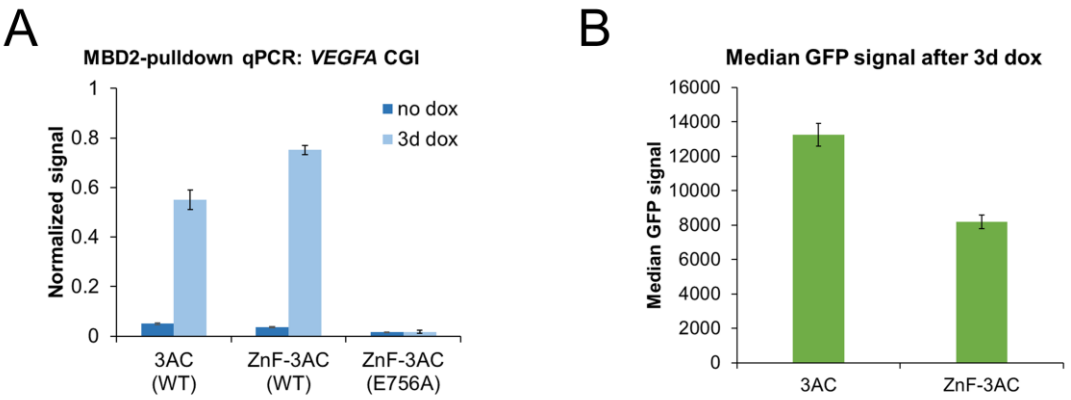

Supplementary Figure S7: Additional controls regarding the ZnF targeting of methylation. (**A**) Targeting of 3AC via zinc finger fusion leads to higher methylation compared to untargeted 3AC without zinc finger. The diagram shows a qPCR analysis of a region in the *VEGFA* promoter CGI 7 bp downstream of a zinc finger binding motif in the MBD2-pulldown samples. The qPCR signals were first normalized to input and then internally re-normalized to the almost fully methylated CGI in the *SLC6A3* promoter. In all cases, the *VEGFA* promoter CGI is unmethylated at no dox. ZnF fusion to 3AC leads to 36% higher signal compared to 3AC alone. For the catalytically inactive mutant E756A no gain in methylation was observed. Bars show the average of two biological replicates, error bars indicate the standard deviations. (**B**) Median signal of GFP co-expressed with 3AC or ZnF-3AC after 3d dox induction. Error bars indicate the standard deviation of three biological experiments.

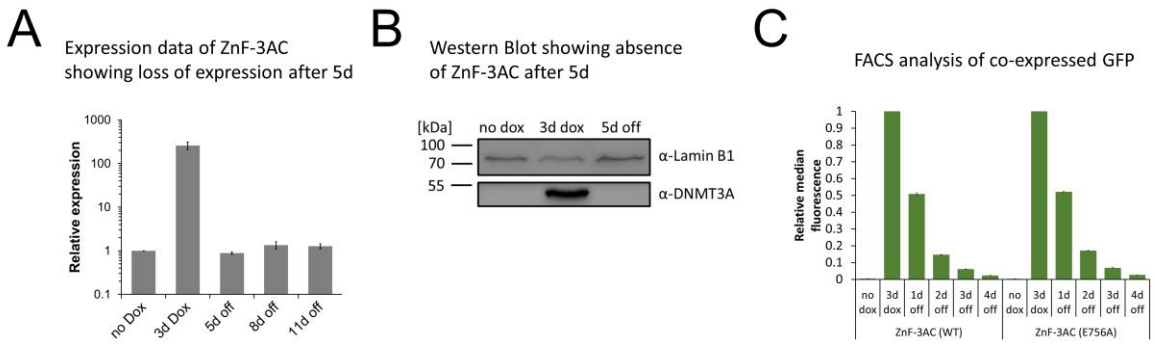

Supplementary Figure S8: Expression of ZnF-3AC rapidly returns to baseline levels after dox removal and does not lead to the counter-selection of highly expressing cells. (**A**) RT qPCR for ZnF-3AC normalized to the non-CGI gene *RAB13* at different time points and shown as relative expression to the 'no dox' state. Error bars indicate the standard deviation of two replicates. (**B**) Western Blot of whole cell lysates at time points 'no dox', '3d dox' and '5d off' showing the absence of ZnF-3AC five days after dox removal. Lamin B1 was used as a loading control. (**C**) GFP is co-expressed with ZnF-3AC wild type or the catalytically inactive E756A mutant. Cells were sorted after 3 days of dox treatment and medians of GFP in flow cytometry were determined. Fractions of the sorted cells were grown until 4 days after sorting without dox treatment and GFP signals were measured every day. For three replicates per time point, means were calculated from medians and plotted in the diagram. The identical time course in the decline of GFP expression in both samples indicates that active DNMT3AC does not lead to a counter-selection when compared to catalytically inactive DNMT3AC. Error bars indicate the standard deviation.

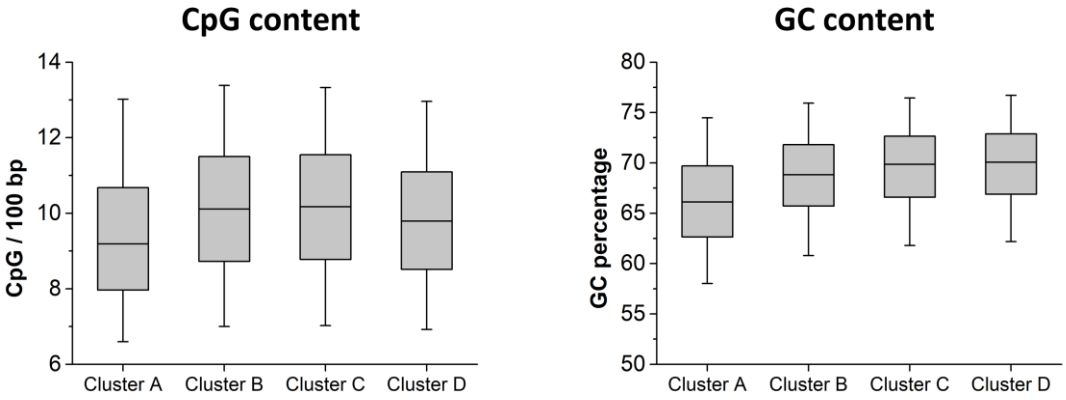

Supplementary Figure S9: Distribution of the CpG density (CpGs per 100 bp) and GC content in the CpG islands from clusters A - D. The line in the box indicates the median, the box indicates the 25th and 75th percentile, the whiskers the 5th and 95th percentile.

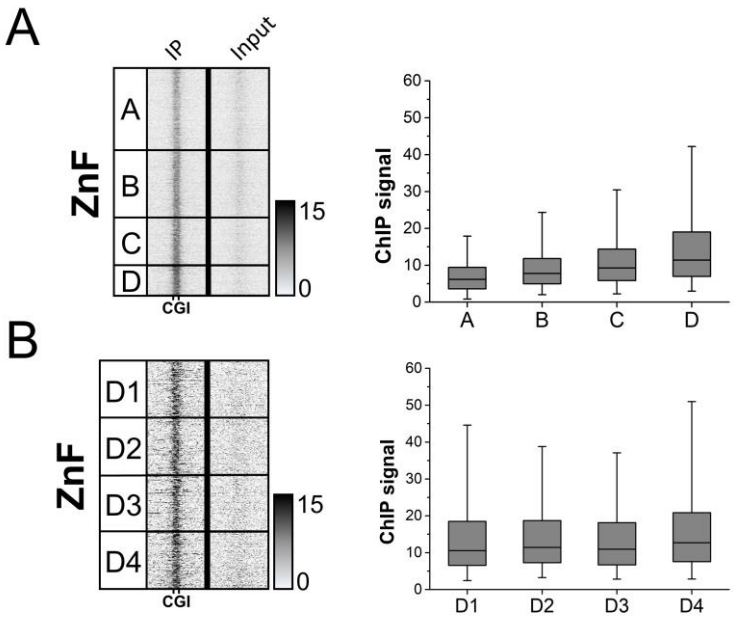

Supplementary Figure S10: ZnF-ChIP signals in differentially methylated clusters. The zinc finger is fused to a triple HA-tag and an antibody against HA-tag was used in XChIP. The heatmaps are centered around CGIs with 5 kb flanks and XChIP-input was plotted besides. The line in the box indicates the median, the box indicates the 25th and 75th percentile, the whiskers the 5th and 95th percentile. ZnF binding was analyzed for (**A**) the main clusters A – D and (**B**) the subclusters D1 – D4.

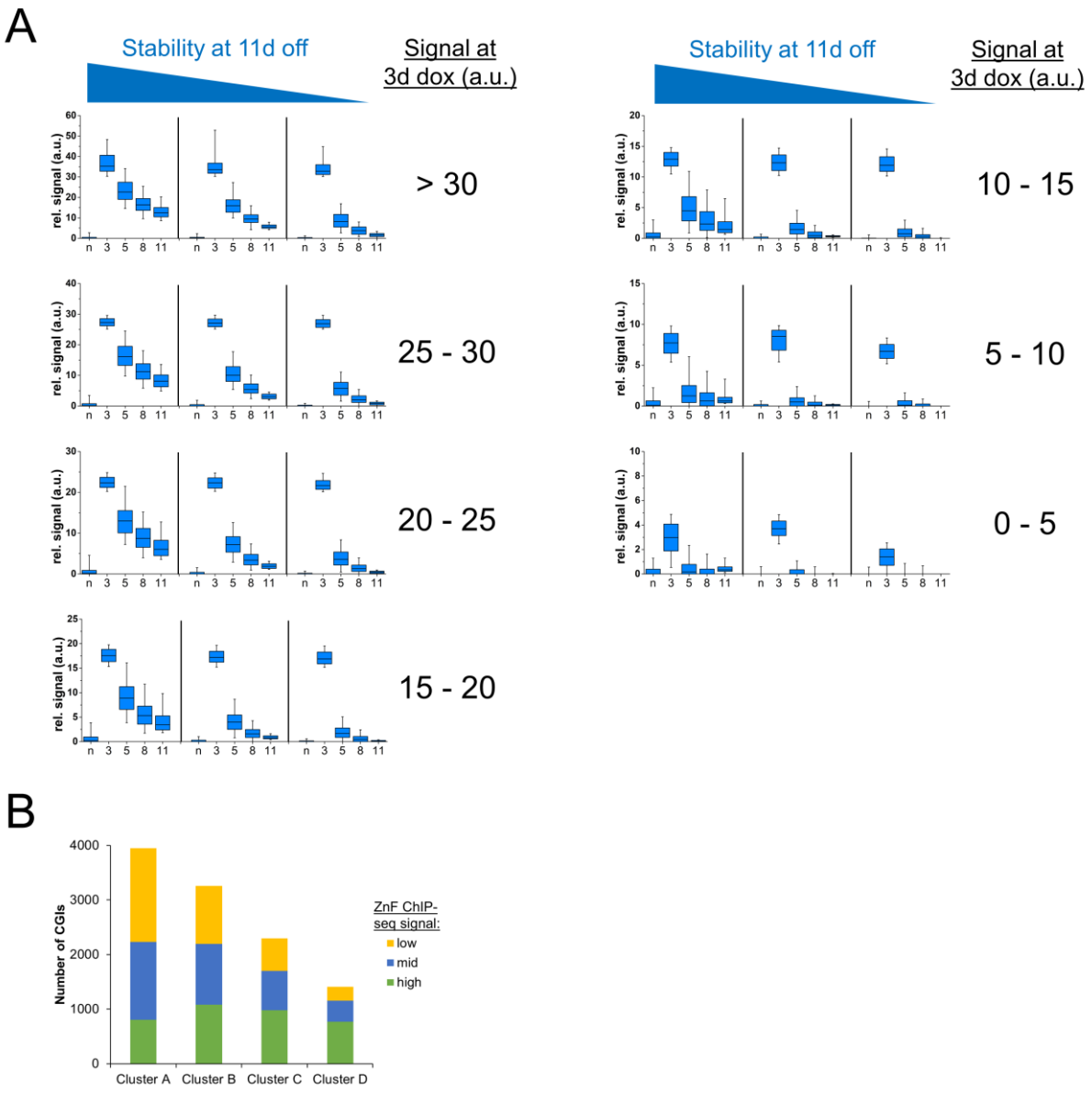

Supplementary Figure S11: Additional analyses regarding the stability of DNA methylation. (**A**) CpG islands with similar methylation levels at '3d dox' show differential loss of methylation over time. CGIs were grouped based on their methylation level at '3d dox' in steps of 5 (a.u.) and within these groups, the relative stability at 11d off was calculated. Based on this, the groups were split into three subgroups of the same size and the signals were displayed in boxplots (from left to right). Although the grouped CGIs showed comparable methylation levels at '3d dox', the stability of the modification highly varies. The line in the box indicates the median, the box indicates the 25th and 75th percentile, the whiskers the 5th and 95th percentile. (**B**) Strong ZnF binding is supportive but not sufficient for stable DNA methylation. CGIs were subdivided into three groups based on the ZnF ChIP-seq signal. Cluster D shows an enrichment in CGIs with high ZnF binding, but high ZnF binding was also observed in Clusters A-C.

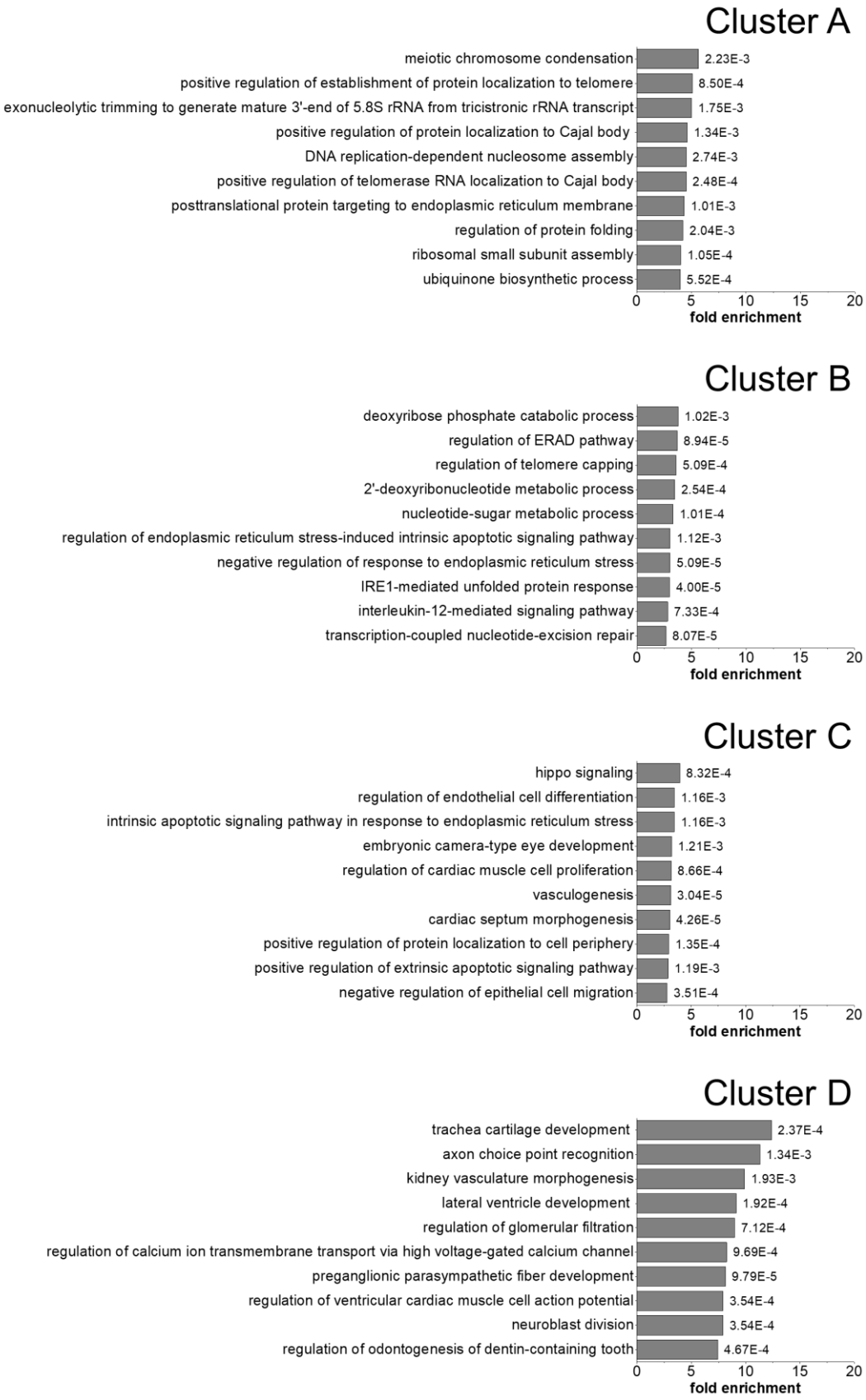

Supplementary Figure S12: Gene ontology analysis of clusters A - D connecting the associated genes to biological processes. The analysis was performed using the http://geneontology.org/ website and the calculated p-values are displayed next to the bars.

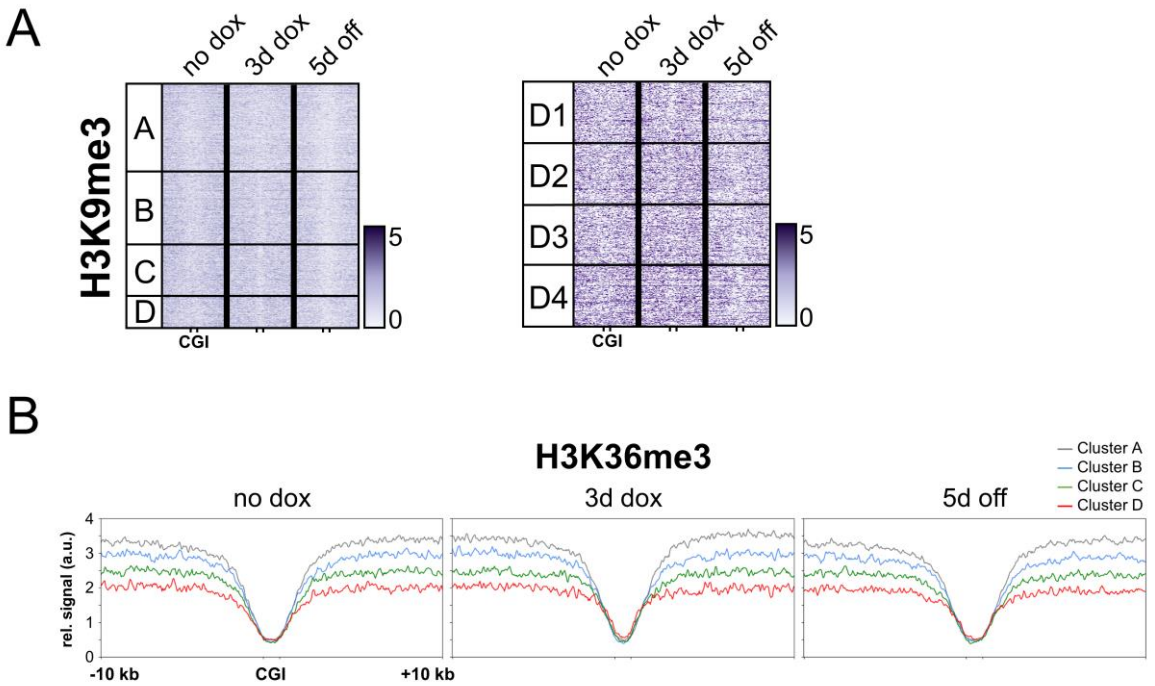

Supplementary Figure S13: The introduction of DNA methylation does not affect H3K9me3 and H3K36me3 levels in CGIs and neighboring gene bodies. (**A**) The heatmaps for H3K9me3 are centered around CGIs with 5 kb flanks. The same clusters and sub-clusters as for MBD2-seq are displayed. No deposition or enrichment of H3K9me3 can be observed. (**B**) Profiles of H3K36me3 signals in clusters A – D are shown. The profile is centered around CGIs with flanks of 10 kb, reaching into the gene bodies of associated genes. No strong effects of DNA methylation on H3K36me3 can be observed neither in the CGIs nor in the gene bodies.

Supplementary tables

Supplementary Table S1: Primers used for MBD2-pulldown qPCR.

Region	Fwd. primer	Rev. primer
VEGFA CGI	GCTTGCCATTCCCCACTTGAATCG	GGTCACTCACTTTGCCCCTGTC
SLC6A3 CGI	GCACTCGCCTAAGAAAACCA	GGAAGGAAAGCCTCGGAGT

Supplementary Table S2: Primers used for RT qPCR.

Gene	Fwd. primer	Rev. primer
ZnF-3AC	TAGACACCAACGTACTCACACCGGTC	GCAATGTAGCGGTCCACTTGG
RAB13	CTCGAGAGCATGGAATCCGA	AGGTCAGTACTGGGAGGCTT

Supplementary Table S3: Primers used for bisulfite sequencing.

Amplicon	Fwd. primer	Rev. primer with barcode *(BC)*
NRP1_1	GTTTGTAATTGTTTGATAGGAGATTGGG	(*BC)*GCCTACAAAAACTACCCAACTCTCCCTC
NRP1_2	AGAGGGAGAGTTGGGTAGTTTTTG	(*BC)*ACAACGACACTACTACCCCTC
VEGFA_1	TTAGGTTGTGAATTTTGGTGGGGG	(*BC)*GAACCTCAACCCTTCCACAC
VEGFA_2	GGAGTTATGCGTTTTTTTTTTTTTTTTTTAAAAG	(*BC)*AAATAAAACCCGAATCAATAAATATCAAATTCC
VEGFA_3	GTTTGTTATTTTTTATTTGAAT	(*BC)*AATCACTCACTTTACCCCTATC
VEGFA_4	GAGTTTGGGAAAAGTTTTGGGGTGGATTGTTG	(*BC)*GCCACTCTAAACTCCCCATTC
EFCAB2_1	GAGAAGGATAGGGAAGGTAAGGTAGGGGAG	(*BC)*GAATAACCCCCTCCTCAAACC
EFCAB2_2	GGGTTGGTTTTATTATTTTTTTGGGAGTTTAG	(*BC)*GATCCCCAACCCCTCCTTTCCCTTATTTC
UBTF	GTTTTAGCGGTTTTTTTTTTGGTTTTGAGTGG	(*BC)*CGAAAAACAACAAACAACAACCACAACC
THAP1	GCGTAGGGTTTTTATTTGTGGAAAG	(*BC)*CAACAAAACGAACACACTAATCACCCCC
SLC6A3	GAGGTTTTTTAGGTTTAGTTTT	CCTAAAAACTCCATTCCTCC

Supplementary Table S4: Coordinates of browser views shown in Figure 3

Locus	Coordinates in hg19
DLD	chr7:107529070-107534800
JAGN1	chr3:9930993-9934866
NADSYN1	chr11:71159933-71169460
PAIP2	chr5:138674446-138680913
EFCAB2	chr1:245129888-245138615
PGM1	chr1:64058289-64065382
EED	chr11:85951568-85966467
TP53BP2	chr1:224029180-224036038
NOTCH2	chr1:120608319-120614700
UBTF	chr17:42294697-42302629
BRAF	chr7:140620616-140625952
NRBF2	chr10:64891753-64895108
VANGL2	chr1:160367589-160380650
QPCT	chr2:37568274-37576402
DNAH14	chr1:225114119-225120143
IVNS1ABP	chr1:185280675-185290476

Supplementary Table S5: Coordinates of browser views shown in Figure 6

Locus	**Coordinates in hg19**
CCND2	chr12:4351974-4416537
SHH	chr7:155590974-155606416
NIM1K	chr5:43186397-43207992
OVOL2	chr20:18030767-18045144

Supplementary Table S6: Coordinates of browser views shown in Supplementary Figure S1

Locus	**Coordinates in hg19**
NRP1	chr10:33622300-33626746
VEGFA	chr6:43736600-43740600
EFCAB2	chr1:245129516-245136513
UBTF	chr17:42294967-42301196
THAP1	chr8:42697749-42698962
SEC24C	chr10:75503613-75504598
SLC6A3	chr5:1443909-1447226

Supplementary Text

Supplementary Text S1: Nucleotide and protein sequence of the ZnF-3AC (wildtype) construct. The catalytic domain of DNMT3A (3AC; green) originates from *Mus musculus* and its protein sequence is identical to human 3AC. The zinc finger (ZnF) sequence is highlighted in yellow, the two nuclear localization sequences are shown in purple and the FLAG tag is in light blue.

Nucleotide sequence (ZnF-3AC):

ATGGGCCCAAAGAAGAAGAGAAAAGTTACCGGGGAGAAGCCCTATGCTTGTCCGGAATGTGGTAAGTCCTTC
AGCGATAGAAGTAATCTGACAAGACACCAGCGTACCCATACGGGTGAAAAACCGTATAAATGCCCAGAGTGC
GGCAAGTCTTTCAGTATGAGTCATCATCTGAGTAGACATCAACGCACCCACACTGGCGAGAAGCCATACAAAT
GTCCAGAATGTGGCAAGTCCTTCTCTAGAAGTGATCATCTGAGTAGACACCAACGTACTCACACCGGTCGGAA
TTCCGGCCCAAAAAAGAAGAGAAAGGTCGACGGCGGTGGATCCAACCATGACCAGGAATTTGACCCCCCAAA
GGTTTACCCACCTGTGCCAGCTGAGAAGAGGAAGCCCATCCGCGTGCTGTCTCTCTTTGATGGGATTGCTACA
GGGCTCCTGGTGCTGAAGGACCTGGGCATCCAAGTGGACCGCTACATTGCCTCCGAGGTGTGTGAGGACTCC
ATCACGGTGGGCATGGTGCGGCACCAGGGAAAGATCATGTACGTCGGGGACGTCCGCAGCGTCACACAGAA
GCATATCCAGGAGTGGGGCCCATTCGACCTGGTGATTGGAGGCAGTCCCTGCAATGACCTCTCCATTGTCAAC
CCTGCCCGCAAGGGACTTTATGAGGGTACTGGCCGCCTCTTCTTTGAGTTCTACCGCCTCCTGCATGATGCGCG
GCCCAAGGAGGGAGATGATCGCCCCTTCTTCTGGCTCTTTGAGAATGTGGTGGCCATGGGCGTTAGTGACAAG
AGGGACATCTCGCGATTTCTTGAGTCTAACCCCGTGATGATTGACGCCAAAGAAGTGTCTGCTGCACACAGGG
CCCGTTACTTCTGGGGTAACCTTCCTGGCATGAACAGGCCTTTGGCATCCACTGTGAATGATAAGCTGGAGCTG
CAAGAGTGTCTGGAGCACGGCAGAATAGCCAAGTTCAGCAAAGTGAGGACCATTACCACCAGGTCAAACTCT
ATAAAGCAGGGCAAAGACCAGCATTTCCCCGTCTTCATGAACGAGAAGGAGGACATCCTGTGGTGCACTGAA
ATGGAAAGGGTGTTTGGCTTCCCCGTCCACTACACAGACGTCTCCAACATGAGCCGCTTGGCGAGGCAGAGAC
TGCTGGGCCGATCGTGGAGCGTGCCGGTCATCCGCCACCTCTTCGCTCCGCTGAAGGAATATTTTGCTTGTGTG
TCTAGAGACTACAAAGACGATGACGACAAGTGA

Protein sequence (ZnF-3AC):

MGPKKKRKVTGEKPYACPECGKSFSDRSNLTRHQRTHTGEKPYKCPECGKSFSMSHHLSRHQRTHTGEKPYKCPEC
GKSFSRSDHLSRHQRTHTGRNSGPKKKRKVDGGGSNHDQEFDPPKVYPPVPAEKRKPIRVLSLFDGIATGLLVLKDL
GIQVDRYIASEVCEDSITVGMVRHQGKIMYVGDVRSVTQKHIQEWGPFDLVIGGSPCNDLSIVNPARKGLYEGTGR
LFFEFYRLLHDARPKEGDDRPFFWLFENVVAMGVSDKRDISRFLESNPVMIDAKEVSAAHRARYFWGNLPGMNRP
LASTVNDKLELQECLEHGRIAKFSKVRTITTRSNSIKQGKDQHFPVFMNEKEDILWCTEMERVFGFPVHYTDVSNMS
RLARQRLLGRSWSVPVIRHLFAPLKEYFACVSRDYKDDDDK*